

## Investigation of Schiff Base N, N'-bis (Salicylidene-1, 2-Diaminoethane (Salen) as corrosion inhibitor for Mild Steel in $H_3PO_4$ Solution

M.Murugaiyan<sup>1</sup>, P.Madhu<sup>1</sup>, P.Vennila<sup>1</sup>, G.Venkatesh<sup>2</sup>

<sup>1</sup>Department of Chemistry, Thiruvalluvar govt arts college, Rasipuram, Tamilnadu, India.

<sup>2</sup>Department of Chemistry VSA Group of Institutions, Salem, Tamilnadu, India

**Abstract:** The electrochemical behavior of mild steel was investigated using Schiff base compound, namely N,N'-bis(Salicylidene-1,2-Diaminoethane (Salen) as a corrosion inhibitor in the presence of 1N Phosphoric acid by weight loss method and potential dynamic polarization methods at 303K-333K.. The weight loss study showed that the inhibitor efficiency, increased with increase concentration of inhibitor and variable temperature. The Potentiodynamic polarization study revealed that the Schiff bases acted as mixed type inhibitors. The adsorption of Schiff base inhibitor on mild steel surface in acid obeyed Temkin's, Frumkin, Frundlich adsorption isotherm and Langmuir adsorption isotherm. The Thermodynamic parameters were also calculated to investigate the mechanism of corrosion inhibition. The Surface characteristics of inhibited and uninhibited mild steel samples were investigated by FT-IR and SEM analysis. The electronic properties such as  $E_{HOMO}$ ,  $E_{LUMO}$ , energy gap orbital's used DFT at the BLYP/6-31G (d, p) basis set with the inhibiting action of Salen. Quantum chemical calculations revealed the adsorption of molecule onto the surface.

**Keywords:** corrosion inhibition, Schiff Base (Salen), Adsorption, Thermodynamic parameters, DFT.

### 1. Introduction

Among the protection mechanism were attributed to formation an absorbed film on the metal surface, the inhibitor provokes a small corrosion on the surface of metal and also it is absorbed forming a compact protective thin layer the inhibitor forms a precipitate on the surface of the metal, acting on the aggressive medium in such a way to form protective precipitate or to remove aggressive agents. Various organic inhibitors have been studied as corrosion inhibitors .The hetero atoms containing organic compounds such as N, P, S and O have a lone pair of electrons, may interact with the metal substrate through an electron donation mechanism, reducing metal dissolution at the metal –electrolyte interface. Recent studies presented that Schiff bases were effective inhibitors for generalized corrosion of mild steel and copper and its alloys. The processes of Schiff bas synthesis are simple and can easily introduce groups according expected properties. (1-6)

Recent studies revealed that organic compounds containing polar functional groups would be quite efficient in minimizing the effect of corrosion in addition to hetero cyclic compounds contain polar groups and electrons.

DFT focuses on the electron density itself as the carrier of all, information on the molecular ground state. Important molecular properties of molecules such as  $E_{HOMO}$ ,  $E_{LUMO}$ ,  $\Delta E$  gap, dipole movement, etc., have been correlated with the inhibition efficiency of different inhibitors using DFT.

The aim of this study to investigate the inhibitory effect of Schiff base compounds N, N'-bis (Salicylidene-1, 2-Diaminoethane (Salen) on the corrosion of mild steel in 1N H<sub>3</sub>PO<sub>4</sub> using weight loss, Potentiodynamic polarization techniques. The mode of adsorption and the corrosion inhibition and quantum chemical calculation (DFT) also discussed. The surface morphology was investigated by SEM analysis.

## 2. Experimental Details

### 2.1. Sample Preparation

Mild steel specimens (Fe-99.686, Ni-0.01, Mo-0.017, Cr-0.043, S-0.014, P-0.008, Si-0.005, Mn-0.196 and C-0.017%). Rectangular samples of area 5 cm x 1 cm have been cut from a large sheet of mild steel. The samples were polished, drilled a hole at one end and numbered by punching. The surface of specimens was polished with emery papers ranging from 110 to 410 grades and decreased with trichloroethylene specimens were dried and stored in desiccators for further use.

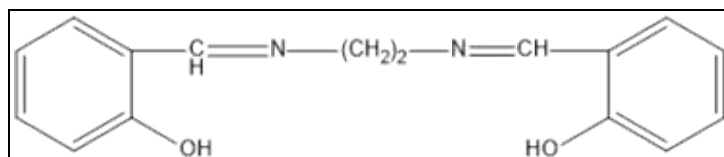
### 2.2. Synthesis of Inhibitor

The Schiff base was prepared by the condensation of respective aromatic aldehydes with each of the domains as per the reported procedure. All reagents used were of analytical grade procured from Sigma Aldrich. N, N'-bis (Salicylidene-1, 2-Diaminoethane (Salen) was prepared by slow addition of salicylaldehyde (2M) in 30 ml methanol over a solution of 1,2 -Diaminomethane (1M) in 30 ml methanol taken in a 250 ml of condensation flask. In each case, 2-3 drops of acetic acid were added to the mixture of aldehydes and Diamon with stirring at constant temperature 298K for 1 hour. The mixture was refluxed for 4-5 hours in a water bath heating occasionally to improve the yield of the product. The reaction mixture was cooled to room temperature overnight and colored compound was filtered off and dried. The compound was recrystallized with ethanol. The product identified was confirmed via melting points, FT-IR, <sup>1</sup>HNMR, the structure, Molecular formula, Molecular mass, Melting points are shown in Table-1. (7-9)

IR (KBr cm<sup>-1</sup>) : 3413(OH), 3036(=C-H), 2863(-CH), 1625(c=N).

<sup>1</sup>HNMR (CDCl<sub>3</sub>):  $\delta$  3.93(s, 4H-CH<sub>2</sub>-N), 6.82-7.4 (m, 8H, ArH), 8.34 (s, N=CH), 13.15(s, 1H, OH)

**Table-1. Schiff Bases**



Structure	N,N'-bis(Salicylidene-1,2 Diaminoethane
Molecular Formula	C <sub>16</sub> H <sub>16</sub> N <sub>2</sub> O <sub>2</sub>
Molecular Mass	268.31
Melting Point	128°C

From the Salen was prepared the various concentrations of inhibitor solution (0.1, 0.2, 0.3, 0.4, and 0.5%). All the solutions were prepared with double distilled water.

### 2.3. Weight loss measurement:

Polished specimens were initially weighed in an electronic balance. After that the specimens were suspended with the help of PTFE threads and glass rod in 100ml beaker containing acid in the presence and absence of Salen. The specimens were removed after 3 hours exposure period, washed with water to remove any corrosion products and finally washed with acetone. After that they were dried and reweighed. Mass loss measurements were carried out in 1N phosphoric acid with ROE in the concentration of 0.1mgs to 0.5mgs as

inhibitor and the temperature between 303K, 313K, 323K, and 333K for an impressive period of 3 hours. Mass loss measurements were performed as per ASTM method described previously. (10)

## 2.4. Potentio dynamic polarization

The potential dynamic measurements were made to evaluate the corrosion current potential, tafel slopes. The polarization measurement has been taken with the help of three electrode system working electrode as mild steel specimen of 5 x 1 cm which was exposed and the rest being covered with red lacquer, a rectangular Pt foil as the counter electrode and the reference electrode as SCE. A time interval of 10-15 minutes were given for each experiment to attain the steady state open circuit potential. The polarization was carried from a cathodic potential of -800 mV to an anodic potential -200mV at a sweep rate of 1mV. From the polarization curves, Tafel slopes, corrosion potential and corrosion current to be calculated. The inhibitor efficiency was calculated from following equation

$$IE\% = \frac{I_{corr} - I^*_{corr}}{I_{corr}} \times 100 \quad \text{-----(1)}$$

Where  $I_{corr}$  and  $I^*_{corr}$  are corrosion current in the absence and presence of inhibitors.

## 2.5. FT-IR Analysis

The corrosion products formed on the steel surface during weight loss measurements were removed by cropping and was used for recording FT-IR spectra. This study reveals the possibility of the adsorption of the inhibitor on the metal surface. The Fourier transform infrared (FT-IR) spectra of the scraped films were recorded using a (Perkin Elmer -1400) FT-IR spectrophotometer.

## 2.6. SEM Analysis

Scanning Electron Microscope uses a focused beam of high energy electron to generate a variety of signals at the surface of solid specimens. The signal that derives from electron –samples, interaction about the sample including external morphology, chemical composition, crystalline structure and orientation of materials making up the sample. An area ranging approximately from 1 cm to 5 microns in width can be imaged in a scanning mode using conventional SEM technique.

## 2.7. Computational Details.

The Density functional theory is one of the most important theoretical model used to analyze the characteristics of the inhibitor/surface mechanism and do describe the structural nature of the inhibitor on the corrosion process. B3LYP a version of the DFT method that uses Beckes three parameter functional (B3) and includes a mixture of HF with DFT exchange terms associated with the gradient corrected correlation functional of Lee, Yang and Parr (LYP) was used in this paper to carry out quantum calculations. The geometry optimization with the vibration analysis of the optimized structures of the inhibitor was carried out at the Gaussian 09 software package of (B3LYP/6-31G(d)) level of theory.

## 3. Result and discussion

### 3.1. Weight loss method

For weight loss experiments, mild steel specimens were immersed in 1N  $H_3PO_4$  solution (100ml) for an optimized time period (3 hours). Effect observed and analyzed by comparing the data obtained without and with different concentration of N, N'-bis (Salicylidene-1, 2-Diaminoethane). Corrosion rate (CR) is directly proportional to the weight loss  $cm^{-2}$  in a specified time and was calculated (mmpy) by the formula.

$$CR = \frac{87.6 \times W}{\rho \times A \times T} \quad \text{----- (2)}$$

Where, W = weight loss in mg,  $\rho$  = density (7.51 g/cm<sup>3</sup> for mild steel) of material used, A = area in cm<sup>2</sup> and t = exposure time in hours.

Table-1 show the value of inhibition efficiency (IE %), surface coverage ( $\theta$ ) and corrosion rate obtained at different concentration of the inhibitors in 1N phosphoric acid solution for an immersion period of 3 hours.

From the mass loss value, the inhibition efficiency (IE%), surface coverage ( $\theta$ ) was calculated using the following equation.

$$IE (\%) = \frac{W_u - W_i}{W_u} \times 100 \text{ ----- (3)}$$

$$\Theta = \frac{W_u - W_i}{W_u} \text{ ----- (4)}$$

Where  $W_0$  and  $W_1$  are the corrosion rates of mild steel in the absence and presence of inhibitor respectively at the same temperature. The inhibition efficiency, increased with increase in concentration of inhibitors and decreased the temperature from 303K to 333K in 1N phosphoric acids shown in Table-2.

**Table-2 Corrosion behavior of mild steel in 1N phosphoric acid with salen at various temperatures (303K -333K)**

S.no	Conc.of Salen (%)	303K		313K		323K		333K	
		CR (mmpy)	I.E(%)	CR (mmpy)	I.E (%)	CR (mmpy)	I.E(%)	CR (mmpy)	I.E (%)
1	Blank	62.38		116.08		136.86		159.18	
2	0.1	39.51	24.69	37.25	12.57	66.26	30.95	73.65	45.26
3	0.2	27.56	35.34	26.06	35.27	41.54	50.14	65.34	52.16
4	0.3	25.95	47.91	24.84	44.96	39.69	58.55	59.00	63.28
5	0.4	22.62	59.43	21.96	49.54	27.69	66.11	44.02	71.41
6	0.5	19.02	63.56	19.56	60.89	16.86	69.93	37.42	76.45

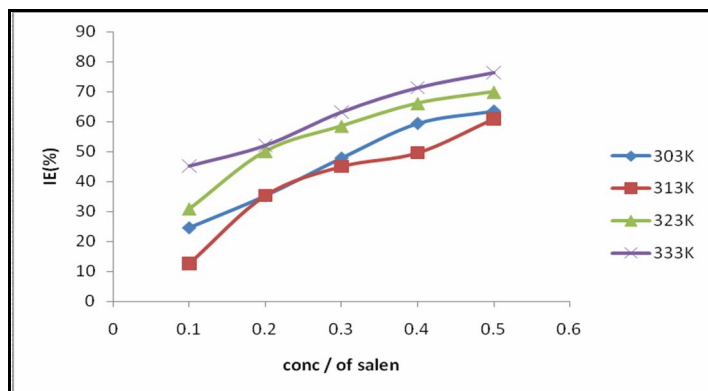


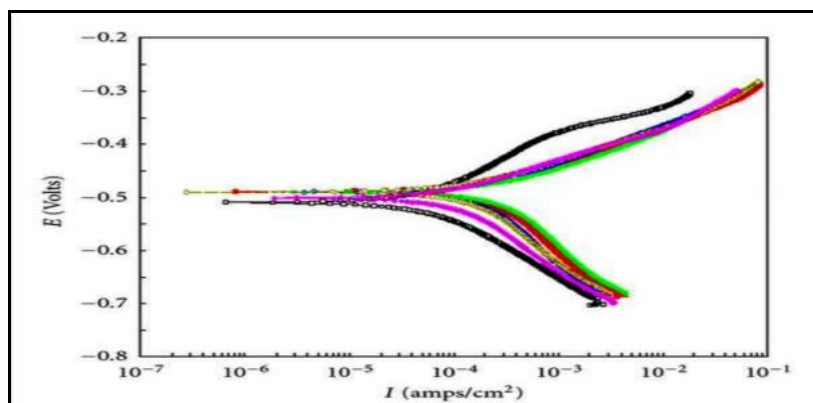
**Figure-1 Corrosion behavior of mild steel in 1N phosphoric acid with Salen at various temperature (303K -333K)**

### 3.2. Potentiodynamic polarization curves

Potential dynamic anodic and cathodic polarization plots for mild steel specimens in 1N phosphoric acid solution in the presence and absence of various concentrations of Salen at 303K are shown in Fig 2. The respective kinetic parameters including current density ( $I_{corr}$ ), current potential ( $E_{corr}$ ) cathodic slopes ( $\beta_c$ ) inhibition efficiency (IE%) are given in Table .3 The analysis of the data revealed that the corrosion current density decrease with increasing the inhibitor concentration and the corrosion potential shifts to less negative values on addition of salen .The value of anodic and cathodic Tafels slopes ( $b_a$  and  $b_c$ ) are slightly changed indicating that this behavior reflects the plant extract ability to inhibit the corrosion of mild steel in 1N  $H_3PO_4$  solution .The adsorption of its molecules on both anodic and cathodic sites and consequently, the salen act through the mixed type inhibition. (11)

**Table 3.** Potentiodynamic polarization parameters for mild steel in 1N H<sub>3</sub>PO<sub>4</sub> containing various concentrations of Salen.

S.NO	Conc. of Salen(%)	E <sub>corr</sub> (V)	I <sub>corr</sub> (mA/cm <sup>2</sup> )	Tafel Slope mV/D		IE(%)
				ba	bc	
1	blank	-0.510	3.56	78	125	-
2	0.1	-0.515	0.24	74	122	93.25
3	0.2	-0.498	0.12	76	126	96.62
4	0.3	-0.496	0.10	75	124	97.19
5	0.4	-0.499	0.09	74	122	97.47
6	0.5	-0.500	0.08	76	126	97.75

**Figure 2** Potentiodynamic polarization parameters for mild steel in 1N H<sub>3</sub>PO<sub>4</sub> containing various concentrations of Salen.

### 3.4. Thermodynamic parameters:

Theoretical fitting of the corrosion data to the kinetic thermodynamic model was tested to show the nature of adsorption. Table 4 shows that the calculated values of energy of activation (E<sub>a</sub>) for mild steel corrosion in 1N phosphoric acid with and without inhibitor from 303K to 333K. Energy of activation (E<sub>a</sub>) was calculated from Arrhenius equation.

$$\log \left( \frac{CR_2}{CR_1} \right) = E_a / 2.303R \left[ \frac{1}{T_1} - \frac{1}{T_2} \right] \quad \text{----- (6)}$$

Where CR<sub>1</sub> and CR<sub>2</sub> are corrosion rates of mild steel at the temperatures T<sub>1</sub> (303K) and T<sub>2</sub> (313K) respectively. The free energy of adsorption [ΔG<sub>(ads)</sub>] was calculated from the following equation

$$\Delta G_{(ads)} = -RT \ln (55.5K) \quad \text{----- (7)}$$

And K is given by

$$K = \theta / C (1 - \theta) \quad \text{----- (8)}$$

Where θ is surface coverage, C is the concentration of inhibitor (salen) and K is the equilibrium constant.

The enthalpy of adsorption (ΔH) was calculated using the equation

$$\Delta H = E_a - RT \quad \text{----- (9)}$$

The entropy of adsorption (ΔS) was calculated using the equation

$$\Delta G = \Delta H - T\Delta S \quad \text{----- (10)}$$

**Table-4** Thermodynamic parameters for mild steel in 1N phosphoric acid with salen at various temperatures (303K -333K)

S.No	Conc. (mgs)	E <sub>a</sub> KJ/mole	ΔH KJ/mole	ΔS KJ/mole	-ΔG <sub>ads</sub> (KJ/mole)			
					303K	313K	323K	333K
1	Blank	48.96	24.70	-	-	-	-	-
2	0.1	46.43	24.72	0.0383	13.1	11.39	14.81	15.43
3	0.2	44.12	24.75	0.0400	12.61	12.64	15.12	15.81
4	0.3	34.46	24.84	0.0392	12.94	13.05	14.94	15.95

5	0.4	23.34	24.95	0.0381	13.38	12.78	15.04	16.19
6	0.5	22.07	24.97	0.0386	13.26	12.97	14.91	16.29

The calculated values of energy of activation ( $E_a$ ), free energy of adsorption [ $\Delta G_{(ads)}$ ], enthalpy of adsorption ( $\Delta H$ ), the entropy of adsorption ( $\Delta S$ ) are shown in Table 4. Ebenso et al 2003 Was reported that the values of  $E_a > 80$  KJ Mol<sup>-1</sup> indicate chemical adsorption whereas  $E_a < 80$  KJ/Mol infer physical adsorption. The activation energy values support the fact that inhibitors are physical adsorption.

The values of  $\Delta G_{ads}$  around -20KJ Mol<sup>-1</sup> or lower are consistent with the electrostatic interaction between organic charged molecules and charged metal (physisorption) as discussed by merrtti et al 2004. In this case the negative sign of free energy of adsorption ( $\Delta G_{ads}$ ) for salen indicates that the adsorption of the salen on mild steel surface was a spontaneous process band the adsorption could be physisorption. The negative value of enthalpy of adsorption ( $\Delta H$ ) indicates that the reaction was exothermic and adsorption of the inhibitor on the metal surface has taken place. As positive sign of entropy of adsorption ( $\Delta S$ ) indicates that the reaction was spontaneous and feasible.

### 3.5. Applicability of Adsorption isotherms

The surface coverage ( $\theta$ ) values for different concentrations of the inhibitor in acid medium have been evaluated from weight loss data. The data were tested graphically to find a suitable adsorption isotherm. A plot of  $\log (\theta/(1-\theta))$  vs  $\log C$  shows Figure 4 a straight line indicating that adsorption follows the Langmuir adsorption isotherm. It is observed that although these plots are linear the gradients are never unity, contrary to what is expected for ideal Langmuir adsorption isotherm equation. Organic molecules having polar atoms or groups which are adsorbed on the metal surface may interact by mutual repulsion or attraction and this may be advocated as the reason for the departure of slope values from unity. A straight line was obtained when the surface coverage was plotted vs  $\log C$ . This shows that the adsorption obeys a Temkin adsorption isotherm, which is graphically represented in Figure 5. The plots of  $\log \theta$  vs  $\log C$  are shown in Figure 6 The linearity shows that the adsorption of the inhibitor on mild steel surface follows Freundlich adsorption isotherm. (13)

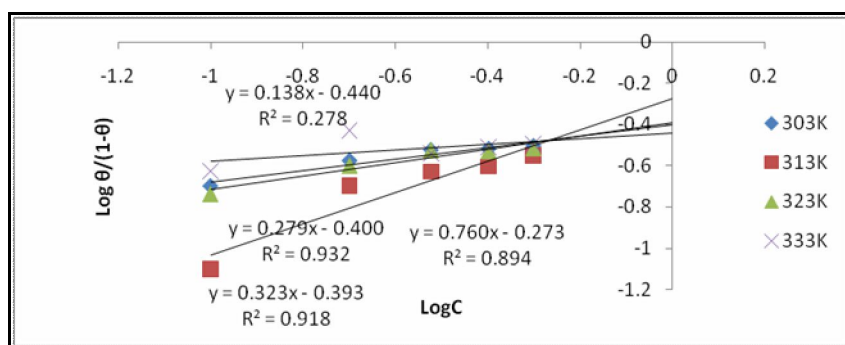


Figure -4Langmuir adsorption isotherm

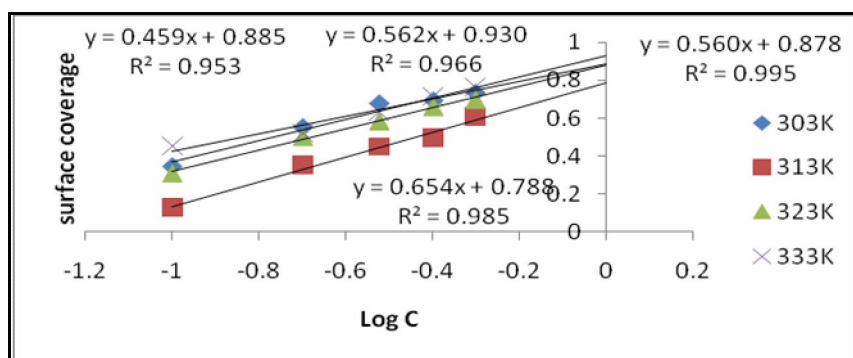


Figure-5 Termkin adsorption isotherm.



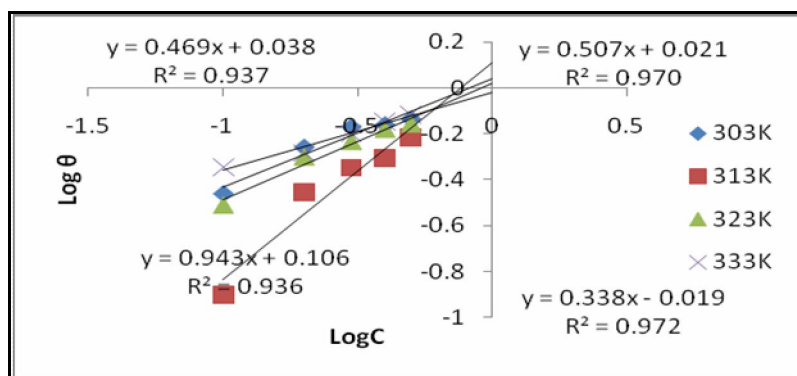


Figure -6 Freundlich adsorption isotherm

### 3.6. Quantum Chemical Calculations:

DFT is very useful technique to probe the inhibitor /surface interaction as well as to analyze the experimental data Figure 7 a to d. Show the optimized geometry, HOMO and LUMO density distribution and total energy for Salen molecules obtained with DFT at B3LYP/6-31G (d, p) level of theory.

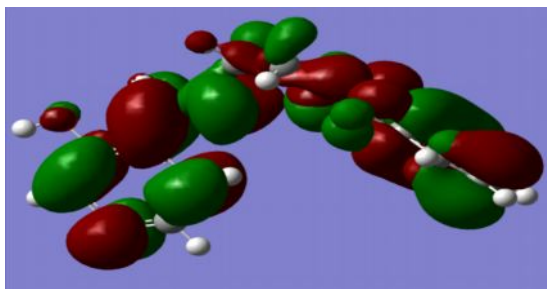
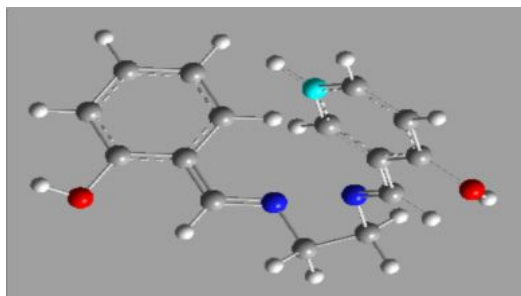
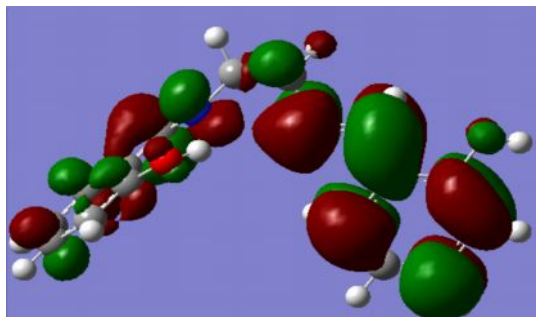
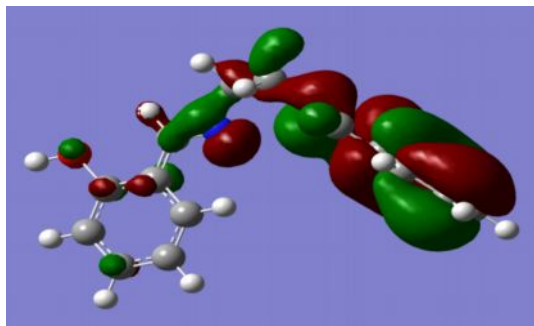


Figure 7 a) Optimization structure for salen

b)HOMO



c) LUMO

d) HOMO-LUMO

Quantum chemical parameters obtained from the calculations which are responsible for the inhibition efficiency of inhibitors, such as the highest occupied molecular orbital ( $E_{\text{HOMO}}$ ) energy of lowest unoccupied molecular orbital ( $E_{\text{LUMO}}$ ),  $E_{\text{HOMO-LUMO}}$  energy gap ( $\Delta E$ ), dipole moment ( $\mu$ ) and total energy are calculated in Table 5

Table 5 Quantum chemical parameters for Salen

S.No	Quantum Parameters	Salen
1	$E_{\text{HOMO}}$	-0.22106au
2	$E_{\text{LUMO}}$	-0.05232au
3	$\Delta E$	-0.16874au
4	Dipole movement (Debye)	1.9141 (Debye)
5	Total energy(TE)	-878.9669au

The inhibition effect of inhibitor compound is usually ascribed to adsorption of the molecule on metal surface. The energy gap  $\Delta E = E_{\text{LUMO}} - E_{\text{HOMO}}$  is an important parameter as a function of reactivity of the inhibitor molecule towards the adsorption on the metallic surface. As  $\Delta E$  decreases, the reactivity of the molecule increases, leading to an increase in the inhibition efficiency of the molecule. Similarly, low values of dipole moment will favor the accumulation of inhibitor molecules on the metallic surface. (14-16). The total energy, calculated by quantum chemical methods is also beneficial parameters. The total energy of a system is composed of the internal, potential and kinetic potential. The total energy of salen is equal is a unique function of the charge density. This is in good agreement with the theoretical and experimental observation suggesting that salen inhibitor molecules have high inhibitor efficiency

### 3.7. FTIR Analysis:

The broad peaks between  $3784.81\text{cm}^{-1}$  and  $3653.25\text{cm}^{-1}$  assigned to the presence of a superficial absorbed water, stretching mode of an OH and  $\text{NH}_2$ . The peak appeared at  $3420\text{cm}^{-1}$  corresponds to  $-\text{OH}$  group, the intensity  $2989.28\text{cm}^{-1}$  is due to N-H stretching vibration of the  $\text{NH}_2$  group. The peaks at  $2888.21\text{cm}^{-1}$ ,  $2819.17\text{cm}^{-1}$  corresponds to stretching vibration of aliphatic and aromatic C-H. The peaks at  $1752.96\text{cm}^{-1}$ ,  $1681.78\text{cm}^{-1}$ ,  $1182.60\text{cm}^{-1}$  corresponds to stretching vibration of C=O; Aromatic substituted C=N, C=C (Aromatic ring), stretching vibration of the ether linkage (C-O) and stretching vibration of C-O. The peaks at  $1481.98\text{cm}^{-1}$  are due to  $\text{NH}_2$  bending vibration. The peaks at  $1310.07\text{cm}^{-1}$  corresponds to C-N symmetric stretching vibration. The C-C-N symmetric stretching vibration is confirmed by the presence of peak at  $909.59\text{cm}^{-1}$ . Then the peaks between  $641.28\text{cm}^{-1}$  and  $496.36\text{cm}^{-1}$  are mainly due to  $\text{Fe}_2\text{O}_3$ . Therefore, from these spectra, it is revealed that the inhibition occurs due to the physical adsorption on the surface of the metal. This is already confirmed from the Langmuir adsorption isotherm studies.

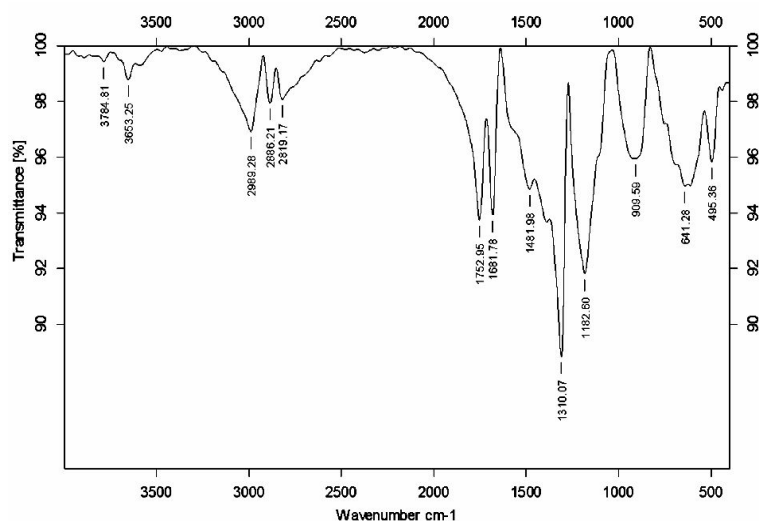


**Fig: 8. FT-IR spectrum of Mild steel in 1N Phosphoric acid with salen**

### 3.8. SEM analysis

Scanning Electron Microscope images were taken in order to study the changes that occur during the corrosion of mild steel in the presence and absence of the green inhibitor Fig -(9a) represents the micro graphs of the mild steel samples after exposure to the corrosive environments. Although they show different morphologies, both portrayed severely damaged surface due to the formation of corrosion products. No pits and cracks are observed in the micro graphs after impression of inhibitors in the corrosive media Fig-(9b) expect polishing lines,. The metal surface was homogeneously covered with the inhibitor molecules. Consequently forming a protective film.



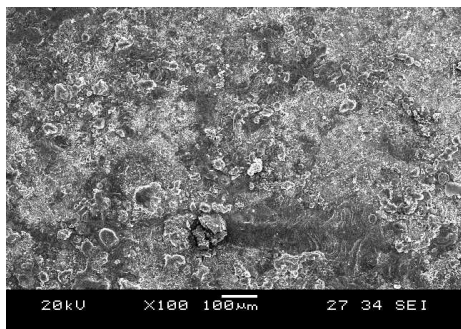


Fig: 9a. SEM analysis of Mild steel in 1N Phosphoric acid

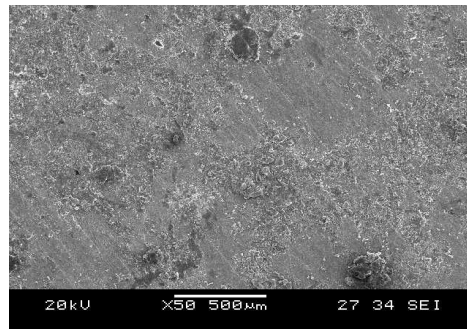
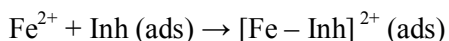
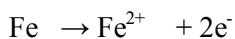


Fig: 9b. SEM analysis of Mild steel in 1N Phosphoric acid with Salen

### 3.9. Mechanism of corrosion inhibition

The inhibitor may then combine with freshly generated  $\text{Fe}^{2+}$  ions on the steel surface, forming metal – inhibitor complexes:



The results obtained so far suggest that the components of the salen exhibited good inhibition efficiency during mild steel corrosion in 1N  $\text{H}_3\text{PO}_4$  solution. The adsorption of the inhibitor molecules on the mild steel surface is due to the donor – acceptor interaction between  $\pi$  electrons of donors atoms O and N, aromatic rings of inhibitors and the acceptor i.e., vacant d orbital of iron surface atoms (17-18). The inhibitor molecules can also be adsorbed on the metal surface in the form of negatively charged species which can interact electrostatically with positive charged metal surface, which led to increase the surface coverage and consequently protect efficiency even in the case of low inhibitor concentration.

## 4. Conclusion

The following conclusion was made from

1. The inhibition efficiency, increased with increase in concentration of salen. The inhibition efficiency obtained from mass loss and polarization measurement also showed fairly good agreement. The Schiff base of salen acts as a mixed type inhibitor.
2. The  $\Delta G_{(\text{ads})}$  value was negative with suggest that they were strongly adsorbed on the metal surface. The Negative values of  $\Delta G_{(\text{ads})}$  indicated the spontaneous adsorption of the inhibitor and were usually characteristic of strong adsorption with the metal.
3. The thermodynamic parameters obtained from the study indicate that the spontaneous adsorption of inhibitor on the surface of the mild steel is an exothermic in nature
4. Adsorption models-Langmuir, Temkin, Frundlich, isotherm fit well as evident from the correlation coefficient values ( $R^2 = 0.9$  in all cases).
5. The inhibitor efficiency of Schiff base quantum chemically increases with the increase in  $E_{\text{HOMO}}$  and decrease  $E_{\text{LUMO}}$ , energy gap. This is in good agreement with the theoretical and experimental observation suggesting that salen inhibitor molecules have high inhibitor efficiency
6. FT-IR and SEM analysis showed the presence of salen compound react with metal ion to form the layer of inhibitor on the metal surface.

## 5. References

1. Kertite, S., Hammouti, B., Appl. Surf. Sci., 93, 59-66., (1996)
2. Quaraish M A., Ansari F. A., Jamal D. M., Mater. Chem. Phys., 77: 687-690 (2002).
3. Chelouani A., Aouniti A., Hammouti B., Benchat N., Corros. Sci., 45, 1675-1684. (2003).
4. Khaled K F., Electrochimica 48, 2493-2503 (2003)
5. Chebabe D., Ati Chiki Z., Hajjaji N., Srhiri A., Zucchi F., Coros. Sci., 45, 309-320 (2003)
6. Wang H., Wang X., Wang L., Liu A., J. Mol., Model., 13, 147., (2007).

7. Sanaulla Pathapalya Fakrudeen.,Lokesh.H B.,Anand Murthy H C.,BheemaRaj.,2012.,Journal of Applied Chemistry., vol 2(5)pp-37-47.
8. Fatemeh Baghaei Revari.,Atharesh Ravari.,Atharesh Dadgarinezhad .,2009.,G.U.journal of science .,vol 22(3).,pp 175-182.
9. Behrouz Shaabani .,Rozhiar Darbari 2013.,Elixir journal of organic chemistry .,vol 55.,pp 12764-12766.
10. Quraishi M A, Khan M A W 2005 .,Journal of Chemical Tech ., 12 .,pp.576-581 .
11. A.,Y.El-Etre 2007 Journal of colloid and interface science ,vol 314.,pp 578-583.
12. Bentiss F, Bouanis M, Traisnel M, Vezin H, Lagrenée M., 2007 .,Applied surface science ., (253)3696 - 3704.
13. Saratha R, Priya S V and Thilagavathy P 2009 ., E-Journal of Chemistry .,vol 6(3) ., pp 785- 795.
14. Udhyakalaa P.,Rajendiranb T V.,Gunasekaranc S.,2012 .,Journal of computational methods in molecular Design.,vol 2(1) pp 1-15.
15. Messali M., Asiri M A M., 2013. Journal of Mater. Environ Sci .,4(5) pp 770-785.
16. Zarroukl A.,Salghi R, Hammouti B., Al-Deyabo S S., A.,2009., Int.J.Electrochem Sci .vol 7.,pp 6353-6364.
17. Stern.M Geary A.L .,1957., J Electrochem Soc., vol 104 ., pp-56 10.1149/1.2428496.
18. Del Bano M.J., .,Lorente .J.,Castillo J.,Benavente-Garcia O.2003.,Journal of Agriculture Biology and Chemistry.,vol.51(10)., pp.42

\*\*\*\*\*